A New pH Oscillator: The Chlorite−Sulfite−Sulfuric Acid System in a CSTR

Glen A. Frerichs,* Tara M. Mlnarik, and Robert J. Grun

Department of Chemistry, Westminster College, Fulton, Missouri 65251

Richard C. Thompson†

Department of Chemistry, University of Missouri-Columbia, Columbia, Missouri 65211

Received: September 18, 2000; In Final Form: November 28, 2000

A new pH oscillator has been discovered involving the system of $NaClO_2$, Na_2SO_3, and H_2SO_4 in a continuous-flow stirred tank reactor (CSTR). While ClO_2^- serves as an oxidant in numerous systems exhibiting nonlinear dynamical behavior, this is the first reported chlorite-based pH oscillator. Large-amplitude oscillations in pH and potential of a platinum electrode were observed over a rather narrow concentration range. Complex dynamical behavior also was observed, including aperiodic oscillations, bistability between steady states, bistability between steady state and oscillatory state, bursting, a possible third steady state, and damped oscillations in batch. Autocatalytic oxidation of HSO_3^- by ClO_2^- is a major source of positive feedback in H^+. A fast Cl^+-transfer reaction between HOCl and SO_3^{2-} is an important source of negative feedback. Oscillations were also obtained in the presence of Na_2CO_3, with the dehydration reaction of H_2CO_3 providing additional negative feedback. Models are proposed to account for observed behavior using computer simulations. Comparisons are made to the ClO_2^-−I^- and ClO_2−I^- oscillating systems, as well as to the general model for chlorite-based chemical oscillators proposed by Rabai and Orban. A possible mechanism for chemical coupling is proposed.

Introduction

Since the discovery of the first pH-regulated chemical oscillator about 15 years ago,[1] the number of pH oscillators has grown rapidly. Recently, some promising ideas for practical applications of pH oscillators have been proposed. One such potential application involves development of temporally controlled drug delivery systems;[2,3] another has to do with simulating the periodic motion of muscular tissue by controlling the mechanical motion of polymer hydrogel systems.[4]

All known pH oscillators have been studied in a continuous-flow stirred tank reactor (CSTR) and require two types of reactions involving H^+: (1) an autocatalytic H^+-producing reaction (positive feedback); (2) an H^+-consuming reaction (negative feedback). These types of reactions have been incorporated into a general model for systematic design of pH oscillators.[5,6]

Typically, mixed Landolt-type systems, involving oxidation of sulfur(IV) species by IO_3^-, BrO_3^-, or H_2O_2, have been used as the autocatalytic reactions. The negative feedback generally has been provided by use of reductants, such as ferrocyanide, thiosulfate, or thiourea (TU), along with the above-mentioned oxidants. Simultaneous H^+-consuming reactions also have been used, such as in the recent application of the enzyme horseradish peroxidase (HRP) to vary the strength of negative feedback in a pH oscillator.[7]

A novel source of negative feedback not requiring a reductant involves carbon(IV) species. Marble chips were used by Rabai and Hanazaki[8] to remove H^+ ions generated by the autocatalytic oxidation of sulfur(IV) by hydrogen peroxide in a CSTR. Rabai[9] later found that marble could be replaced by $NaHCO_3$ in a flow system to produce chaotic pH oscillations, as long as there is controlled removal of the CO_2 formed by reaction of hydrogen carbonate ions with acid.

Frerichs and Thompson[10] reported periodic oscillations, both in pH and in the potential of a Pt electrode, for a homogeneous system in which Na_2CO_3 was used to consume H^+ ions produced by the same positive feedback source as above. The main source of negative feedback in this homogeneous system is the dehydration of H_2CO_3 to give aqueous CO_2. Concentrations of carbon dioxide in the latter case are at less than saturation values, and the CO_2 is not forcibly removed.

Chlorite-based oscillators involving the sulfur-containing species $S_2O_3^{2-}$, SCN^-, S^{2-}, and thiourea have been known for some time.[11−14] A variety of complex dynamical behavior is found in these systems. However, none of these has been reported to be a pH oscillator. Also, the mechanisms for the reactions involved are not well understood. With the goal of designing a new pH oscillator, we considered the possibility of replacing H_2O_2 with ClO_2^- as the oxidant for SO_3^{2-} in the carbonate-based system.

The reaction between chlorite and sulfite ions in acid was first studied by Halperin and Taube.[15] They reported a very rapid reaction, essentially complete in less than one minute at pH 1−5. Attempts by Edblom et al.[16] to obtain oscillations with the chlorite−sulfite−ferrocyanide system were unsuccessful, although bistability was observed.

In the very useful general model for chlorite-based oscillators developed by Rabai and Orban,[17] it is surmised that the failure to obtain oscillations in the chlorite−sulfite system is likely due to the high value of the rate constant for the autocatalytic reaction. No doubt a significant amount of negative feedback

* Corresponding author. E-mail: frericg@jaynet.wcmo.edu. Fax: (573) 642-6356.

† E-mail: thompsonr@missouri.edu. Fax: (573) 882-2754.

10.1021/jp003363u CCC: $20.00
Published on Web 01/12/2001

from carbonate or other sources is required if pH oscillations are to be found.

The chlorite family of oscillators is the largest one known to date, containing several subfamilies (such as the I^-, IO_3^-, and BrO_3^- branches), and accounts for a total of more than two dozen oscillators.[18] The first systematically designed homogeneous chemical oscillator contained chlorite, arsenite, and iodate.[19] Orban et al.[20] reported SO_3^{2-} to be among the reductants giving oscillations with chlorite-based systems involving either IO_3^- or I_2 as oxidants.

One of the most important and best understood of the minimal oscillators of the subfamilies of chlorite oscillators is the chlorite−iodide system. Next to the Belousov−Zhabotinsky (BZ) reaction, the $ClO_2^--I^-$ reaction is perhaps the most widely studied reaction in nonlinear dynamics, over 200 articles having been published on it since 1981.[21]

One of our main goals in this study, in addition to designing a new pH oscillator, is to gain an understanding of the chemical reactions that account for the observed behavior of the system. As will be brought out in the discussion below, we were rather successful in doing this for the $ClO_2^--SO_3^{2-}-CO_3^{2-}-H^+$ system.

As we began to understand better the apparent mechanism for the above system, it occurred to us that pH oscillations possibly could be obtained even without carbonate as a source of negative feedback. This in fact was the case, meaning that the $ClO_2^--SO_3^{2-}-H^+$ system is a new minimal oscillator. As will be discussed below, our proposed model for the oscillatory behavior of this system can be related both to the general model for chlorite reactions and, more specifically, to the mechanism for the chlorite−iodide reaction mentioned above.

Experimental Section

Reagent grade $NaClO_2$, Na_2SO_3, Na_2CO_3, and H_2SO_4 were used without further purification. The $NaClO_2$ source was Matheson, Coleman & Bell (MCB), and was determined by iodometric titration with $Na_2S_2O_3$ to have an assay of 98.2%. All of the other reagents were distributed by Fisher (certified ACS). The Na_2SO_3 had an assay of 99.6% and contained 0.03 meq/g titratable base. The assay of the Na_2CO_3 was 99.9%.

Solutions were prepared using triply distilled water, which was first purged with N_2. Since sulfite is sensitive to oxidation by O_2 in air, Na_2SO_3 solutions were prepared immediately before use. Stock solutions of Na_2CO_3 and H_2SO_4 were prepared, the latter being standardized by titration with standardized NaOH using phenolphthalein as an indicator.

A Plexiglas water-jacketed reactor of volume 43.2 mL was used for all CSTR experiments. The design of the reactor and the procedure for performing a CSTR experiment have been described previously.[10] Reactant solutions were pumped into the reactor through three inlet tubes by means of an IsmaTec digital variable-speed pump with 1% reproducibility of flow rate. A magnetic stirrer was used to ensure uniform mixing. The stirring rate was about 500 rpm.

For experiments with carbonate, $NaClO_2$ and H_2SO_4 were in separate inlet streams, with Na_2SO_3 and Na_2CO_3 in the other stream. In those experiments not involving carbonate, only Na_2SO_3 was in the third inlet stream. Throughout all experiments, the solutions in their reservoirs were bubbled with N_2, but not the reactor itself.

Where possible, both the flow (F) and thermodynamic (T) branches were obtained. Generally, both a strip chart recorder and a MacLab data acquisition unit were used to record both pH and the potential of a Pt electrode vs a calomel reference electrode. All experiments were carried out at 25 °C.

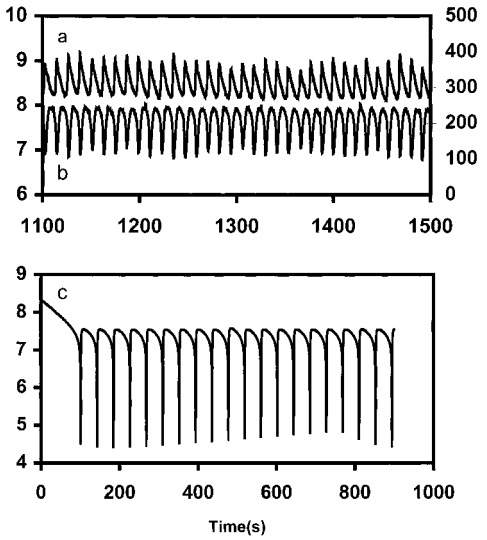

Figure 1. Measured oscillations in potential of a platinum electrode (a) and in pH (b); calculated pH oscillations with rate constants as in Table 2 (c). Input concentrations: $[ClO_2^-]_0 = 5.00 \times 10^{-3}$ M; $[SO_3^{2-}]_0 = 2.00 \times 10^{-3}$ M; $[CO_3^{2-}]_0 = 2.00 \times 10^{-4}$ M; $[H^+]_0 = 3.40 \times 10^{-4}$ M. $k_0 = 1.55 \times 10^{-2}$ s^{-1}.

A number of batch experiments were done, especially to find concentrations where the reaction might give oscillations in a CSTR. The procedure that worked best was first to mix the chlorite and sulfite solutions in the reaction vessel, then quickly to add the sulfuric acid. When the system indicated possible sensitivity to air, later experiments were done under a blanket of N_2 gas.

Results

$NaClO_2-Na_2SO_3-Na_2CO_3-H_2SO_4$ System. As mentioned above, the early experiments were done in the presence of sodium carbonate. The approach used was to vary the amounts of chlorite and sulfite while keeping the carbonate and acid concentrations fixed. Concentrations used were $[CO_3^{2-}]_0 = 2.00 \times 10^{-4}$ M and $[H^+]_0 = 3.40 \times 10^{-4}$ M. This resulted in an $[H^+]_0$:$[CO_3^{2-}]_0$ ratio of 1.70, roughly equal to that used in the study of the homogeneous carbonate-based system involving H_2O_2 as oxidant.[10]

Rapid, large-amplitude, periodic oscillations in pH and potential were obtained using chlorite concentrations in the range: $[ClO_2^-]_0 = 3.00-7.00$ mM. The $[ClO_2^-]_0$:$[SO_3^{2-}]_0$ ratio where oscillations were observed varied from 1.30 (at lower concentrations) to 2.64 (at higher concentrations). The maximum amplitude of observed oscillations under all conditions used was about 1.9 pH units and 210 mV.

Figure 1a,b shows an experimental result obtained in a CSTR with 5.00 mM ClO_2^- and 2.00 mM SO_3^{2-}, along with the above amounts of CO_3^{2-} and H^+. Rather high-frequency oscillations were found, the period ranging from 6 to 8 s at low k_0 (reciprocal residence time) to 10−12 s at high k_0. Also, the k_0 required for oscillations was relatively high, ranging from $(0.6-2) \times 10^{-2}$ s^{-1}.

Often, only SSI or SSII was observed, where SSI is the basic steady state (at high k_0) and SSII is the acidic steady state (at low k_0). Very rapid, small-amplitude, aperiodic oscillations generally occurred about the steady state. Under certain conditions, bistability between SSI and SSII (or even between SSI and the oscillatory state) was found.

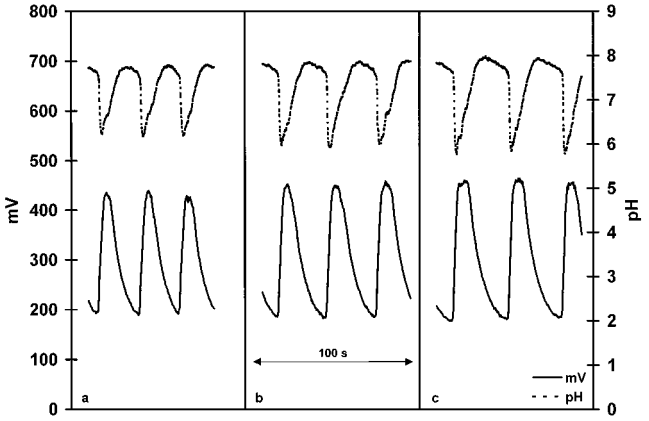

Figure 2. Measured oscillations in potential of a platinum electrode (lower) and in pH (upper). Input concentrations: $[ClO_2^-]_0 = 2.00 \times 10^{-3}$ M; $[SO_3^{2-}]_0 = 1.15 \times 10^{-3}$ M; $[H^+]_0 = 5.04 \times 10^{-5}$ M. $k_0 \times 10^2$, s^{-1}: 1.2 (a); 1.3 (b); 1.4 (c); 1.6 (d); 1.7 (e).

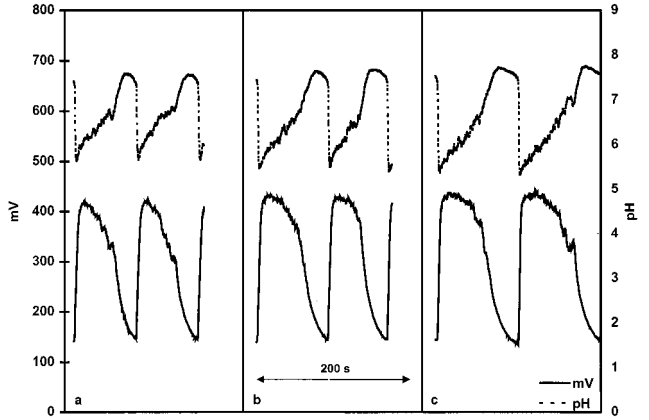

Figure 3. Measured oscillations in potential of a platinum electrode (lower) and in pH (upper). Input concentrations: $[ClO_2^-]_0 = 1.50 \times 10^{-3}$ M; $[SO_3^{2-}]_0 = 8.63 \times 10^{-4}$ M; $[H^+]_0 = 4.42 \times 10^{-5}$ M. $k_0 \times 10^3$, s^{-1}: 7.2 (a); 8.0 (b); 9.2 (c).

It should be mentioned that some difficulty was experienced in duplicating the oscillations experimentally. When it was discovered that carbonate was not necessary in order to obtain oscillations, our attention shifted to the non-carbonate-based system, so this matter was not fully resolved.

$NaClO_2$−Na_2SO_3−H_2SO_4 System. In the non-carbonate-based system, regular, large-amplitude oscillations in pH and potential were found in both the F- and T-branches over a limited concentration range. It was necessary to use somewhat lower concentrations of reactants than in the presence of carbonate. The range of $[ClO_2^-]_0$ giving oscillations was 1.25−4.00 mM. In all cases where oscillations were observed, the $[ClO_2^-]_0$:$[SO_3^{2-}]_0$ ratio was 1.74. The range of $[H^+]_0$ required was $(3.13-8.98) \times 10^{-5}$ M. Typically, the $[SO_3^{2-}]_0$:$[H^+]_0$ ratio used was 22.8, with a range of 20−28.

Compared to the carbonate-based oscillator, the oscillations in this system are of larger amplitude and longer period. The largest amplitudes observed were nearly 2.5 pH units and 420 mV. Periods generally ranged from about 30−120 s. Oscillations in the F-branch usually were found at lower k_0 values ($<5 \times 10^{-3}$ s^{-1}), while those in the T-branch were at higher k_0 ($>6 \times 10^{-3}$ s^{-1}).

Figures 2 and 3 show oscillations in pH and potential for two different CSTR experiments. The nature of the peaks varies considerably with the conditions. Compare the relatively sharp symmetrical peaks found in Figure 2 to the rather broad unsymmetrical peaks in Figure 3. Of special note is the bursting behavior shown in the latter peaks on the return to SSI. Interestingly, expansion of the curves in Figure 2 reveals similar bursting behavior, but on an accelerated time scale.

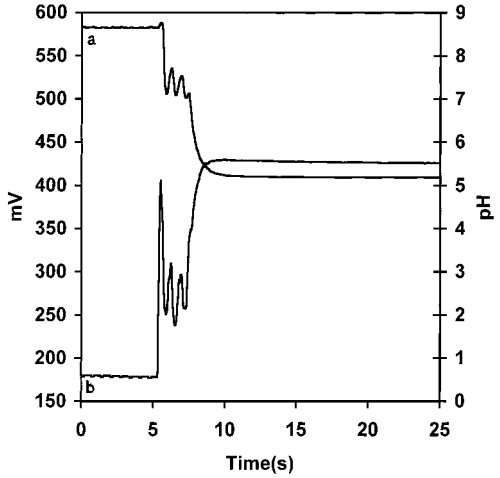

Figure 4. Measured responses in pH (a) and in potential of a platinum electrode (b) for batch reaction. Reactant concentrations: $[ClO_2^-]_0 = 2.00 \times 10^{-3}$ M; $[SO_3^{2-}]_0 = 1.15 \times 10^{-3}$ M; $[H^+]_0 = 3.16 \times 10^{-5}$ M.

In addition to the bursting effect, other complex dynamical behavior was observed in the chlorite−sulfite pH oscillator. Bistability was found, not only between SSI and SSII but also between SSI and the oscillatory state. Aperiodic oscillations often occurred in one branch or the other. In certain instances there appeared to be evidence for birhythmicity.

Another unusual phenomenon for which there is some evidence is the possible existence of a third steady state, SSIII. In more than one experiment, shortly after the T-branch was started at a very low flow rate, the pH increased to 9.5−10. This range is at least one pH unit higher than that generally found for SSI. Where this was observed, the pH eventually dropped significantly and either periodic or aperiodic oscillations between SSI and SSII ensued.

Finally, another rare observation was made in studying the batch reaction. Damped oscillations in pH and potential were obtained. The number of peaks observed ranged from 2 to 4, depending on reactant concentrations. Figure 4 shows the results of a batch experiment using the same concentrations of ClO_2^- and SO_3^{2-} as in the CSTR run corresponding to Figure 2. A lower concentration of H^+ was required in the batch reaction, however. Although batch oscillations were found under various conditions, the rapidity of the reactions made it difficult to duplicate the results quantitatively.

Discussion

$NaClO_2$−Na_2SO_3−Na_2CO_3−H_2SO_4 System. One approach to simulating the carbonate-based pH oscillator is to model it after the corresponding system where H_2O_2 is the oxidant,[10] rather than ClO_2^-. The mechanism proposed for this system is given in Table 1 and consists of chlorite−sulfite subsystem A and the carbonate subsystem. Corresponding rate equations and rate constants are found in Table 2.

Reactions 1, 8, and 9 from chlorite−sulfite subsystem A all involve oxidation of S(IV) species by ClO_2^- in reactions that parallel those with H_2O_2 as oxidant. The values for rate constants k_1, k_8, and k_9 were not available in the literature, but have been determined recently by Rushing and Thompson.[22] It may be noted that k_8 and k_9 are about 7 and 15 times as large, respectively, as their counterparts with H_2O_2 as oxidant.[10] On the other hand, k_1 is difficult to measure because of the slowness

TABLE 1: Reaction Mechanism for the Chlorite−Sulfite−Carbonate pH Oscillator

no.	reaction
	Chlorite−Sulfite Subsystem A
(1)	$ClO_2^- + SO_3^{2-} \rightarrow OCl^- + SO_4^{2-}$
(2)	$OCl^- + H^+ \leftrightarrow HOCl$
(3)	$HOCl + SO_3^{2-} \leftrightarrow HOClSO_3^{2-}$
(4)	$HOClSO_3^{2-} \rightarrow ClSO_3^- + OH^-$
(5)	$ClSO_3^- + H_2O \rightarrow Cl^- + 2H^+ + SO_4^{2-}$
(6)	$OH^- + H^+ \leftrightarrow H_2O$
(7)	$SO_3^{2-} + H^+ \leftrightarrow HSO_3^-$
(8)	$ClO_2^- + HSO_3^- \rightarrow HOCl + SO_4^{2-}$
(9)	$ClO_2^- + HSO_3^- + H^+ \rightarrow OCl^- + 2H^+ + SO_4^{2-}$
	Carbonate Subsystem
(10)	$CO_3^{2-} + H^+ \leftrightarrow HCO_3^-$
(11)	$HCO_3^- + H^+ \leftrightarrow H_2CO_3$
(12)	$H_2CO_3 \leftrightarrow CO_2 + H_2O$

TABLE 2: Rate Equations and Rate Constant Values for the Chlorite−Sulfite−Carbonate pH Oscillator

rate equations	rate constants at 25 °C	ref
	Chlorite−Sulfite Subsystem A	
$R_1 = k_1[ClO_2^-][SO_3^{2-}]$	$k_1 = 1.2 \times 10^{-2}\ M^{-1}\ s^{-1}$	22
$R_2 = k_2[OCl^-][H^+]$	$k_2{}^a = 1 \times 10^{11}\ M^{-1}\ s^{-1}$	38
$R_{-2} = k_{-2}[HOCl]$	$k_{-2}{}^a = 3 \times 10^3\ s^{-1}$	38
$R_3 = k_3[HOCl][SO_3^{2-}]$	$k_3 = 5.0 \times 10^9\ M^{-1}\ s^{-1}$	23
$R_{-3} = k_{-3}[HOClSO_3^{2-}]$	$k_{-3} = 5.6 \times 10^6\ s^{-1}$	23
$R_4 = k_4[HOClSO_3^{2-}]$	$k_4 = 1.0 \times 10^6\ s^{-1}$	23
$R_5 = k_5[ClSO_3^-]$	$k_5 = 2.7 \times 10^2\ s^{-1}$	23
$R_6 = k_6[OH^-][H^+]$	$k_6 = 1.0 \times 10^{11}\ M^{-1}\ s^{-1}$	10
$R_{-6} = k_{-6}[H_2O]$	$k_{-6}[H_2O] = 1.0 \times 10^{-3}\ M\ s^{-1}$	10
$R_7 = k_7[SO_3$2-$][H^+]$	$k_7 = 5.0 \times 10^{10}\ M^{-1}\ s^{-1}$	10
$R_{-7} = k_{-7}[HSO_3^-]$	$k_{-7} = 3.0 \times 10^3\ s^{-1}$	10
$R_8 = k_8[ClO_2^-][HSO_3^-]$	$k_8 = 24.7\ M^{-1}\ s^{-1}$	22
$R_9 = k_9[ClO_2^-][HSO_3^-][H^+]$	$k_9 = 2.19 \times 10^8\ M^{-2}\ s^{-1}$	22
	Carbonate Subsystem	
$R_{10} = k_{10}[CO_3^{2-}][H^+]$	$k_{10} = 1 \times 10^{11}\ M^{-1}\ s^{-1}$	10
$R_{-10} = k_{-10}[HCO_3^-]$	$k_{-10} = 4.8\ s^{-1}$	10
$R_{11} = k_{11}[HCO_3^-][H^+]$	$k_{11} = 5 \times 10^{10}\ M^{-1}\ s^{-1}$	10
$R_{-11} = k_{-11}[H_2CO_3]$	$k_{-11} = 8.6 \times 10^6\ s^{-1}$	10
$R_{12} = k_{12}[H_2CO_3]$	$k_{12} = 16.5\ s^{-1}$	10
$R_{-12} = k_{-12}[CO_2]$	$k_{-12} = 4.3 \times 10^{-2}\ s^{-1}$	10

[a] Based on $K_a = 3.0 \times 10^{-8}$ M for HOCl.

of reaction 1, and is about 17 times smaller than the corresponding rate constant for the reaction involving H_2O_2. Reactions 8 and 9 are significant sources of positive feedback, especially the latter reaction, which is autocatalytic in H^+.

The Cl(I) species generated by reactions 1, 8, and 9 serve as a source of additional feedback, both positive and negative. Margerum et al.[23] have measured rate constants for the very fast reaction of HOCl and SO_3^{2-} to form the chlorosulfate ion, $ClSO_3^-$. They propose a mechanism involving reversible Cl^+ transfer to sulfur via the reactive intermediate, $HOClSO_3^{2-}$, which then decomposes to $ClSO_3^-$ and OH^-. This negative feedback is followed by the relatively slow hydrolysis of $ClSO_3^-$, which is accompanied by release of H^+. These processes are represented by reactions 3−5 in Table 1.

Just as in the H_2O_2 system, dehydration of H_2CO_3 (reaction 12) in the carbonate subsystem is the main source of negative feedback. This process causes the acid−base equilibrium reactions 10 and 11 involving HCO_3^- and CO_3^{2-} to shift in the H^+-consuming direction. Reactions 2, 6, and 7 also involve rapid acid−base equilibria in which a similar shift occurs.

The rate equations given in Table 2 were integrated numerically using the previously described SIMULATE program.[10] Calculated oscillations in pH are shown in Figure 1c for the same conditions as those used experimentally. The general features of the experimental oscillations can be simulated rather well, although not quantitatively.

TABLE 3: Reaction Mechanism for the Chlorite−Sulfite pH Oscillator

no.	reaction
	Chlorite−Sulfite Subsystem A reactions 1−9 from Table 1
	Chlorite−Sulfite Subsystem B
(13)	$ClSO_3^- + HOCl \rightarrow Cl_2SO_3 + OH^-$
(14)	$Cl_2SO_3 + H_2O \rightarrow Cl_2 + 2H^+ + SO_4^{2-}$
(15)	$Cl_2 + H_2O \rightarrow HOCl + Cl^- + H^+$
(16)	$Cl_2 + ClO_2^- \rightarrow Cl_2O_2 + Cl^-$
(17)	$ClSO_3^- + ClO_2^- \rightarrow Cl_2O_2 + SO_3^{2-}$
(18)	$Cl_2O_2 + SO_3^{2-} + H_2O \rightarrow 2HOCl + SO_4^{2-}$
(19)	$Cl_2O_2 + ClO_2^- \rightarrow 2^{\bullet}ClO_2 + Cl^-$
(20)	$^{\bullet}ClO_2 + SO_3^{2-} \leftrightarrow ClO_2^- + SO_3^{\bullet-}$
(21)	$SO_3^{\bullet-} + SO_3^{\bullet-} \rightarrow S_2O_6^{2-}$
(22)	$SO_3^{\bullet-} + SO_3^{\bullet-} + H_2O \rightarrow HSO_3^- + H^+ + SO_4^{2-}$

TABLE 4: Rate Equations and Rate Constant Values for the Chlorite−Sulfite pH Oscillator

rate equations	rate constants at 25 °C	ref
	Chlorite−Sulfite Subsystem A rate equations and rate constants from Table 2	
	Chlorite−Sulfite Subsystem B	
$R_{13} = k_{13}[ClSO_3^-][HOCl]$	$k_{13} = 7.5 \times 10^7\ M^{-1}\ s^{-1}$	this work
$R_{14} = k_{14}[Cl_2SO_3]$	$k_{14} = 0.20\ s^{-1}$	this work
$R_{15} = k_{15}[Cl_2]$	$k_{15} = 11.0\ s^{-1}$	32
$R_{16} = k_{16}[Cl_2][ClO_2^-]$	$k_{16} = 2 \times 10^3\ M^{-1}\ s^{-1}$	27
$R_{17} = k_{17}[ClSO_3^-][ClO_2^-]$	$k_{17} = 1.7 \times 10^5\ M^{-1}\ s^{-1}$	this work
$R_{18} = k_{18}[Cl_2O_2][SO_3^{2-}]$	$k_{18} = 9.4 \times 10^7\ M^{-1}\ s^{-1}$	this work
$R_{19} = k_{19}[Cl_2O_2][ClO_2^-]$	$k_{19} = 5.4 \times 10^4\ M^{-1}\ s^{-1}$	32
$R_{20} = k_{20}[^{\bullet}ClO_2][SO_3^{2-}]$	$k_{20} = 2.82 \times 10^6\ M^{-1}\ s^{-1}$	22
$R_{-20} = k_{-20}[ClO_2^-][SO_3^{\bullet-}]$	$k_{-20} = 1.3 \times 10^3\ M^{-1}\ s^{-1}$	24
$R_{21} = 2k_{21}[SO_3^{\bullet-}]^2$	$2k_{21} = 6.2 \times 10^8\ M^{-1}\ s^{-1}$	25
$R_{22} = 2k_{22}[SO_3^{\bullet-}]^2$	$2k_{22} = 1.1 \times 10^9\ M^{-1}\ s^{-1}$	25

Simulated oscillations in pH are obtained over a flow rate range of $k_0 = (0.552-2.14) \times 10^{-2}\ s^{-1}$, which compares favorably with the experimental range given above. Fairly good agreement is found between the calculated and experimental period of oscillations in the middle portion of the k_0 range, but not near the extremes. Calculated k_0 values are too small at the lower end, and too large at the upper end, of the flow rate range.

A comparison of the concentrations of key reaction species is of interest. Calculations show that $[H^+]$, [HOCl], $[H_2CO_3]$, and $[CO_2]$ all increase substantially during an oscillation, while at the same time $[SO_3^{2-}]$, $[HSO_3^-]$, and $[CO_3^{2-}]$ experience a sharp decrease. The $[HOClSO_3^{2-}]$ and $[ClSO_3^-]$ are never very large, but they do show a gradual increase until the oscillation occurs, followed by a more rapid drop about 2 s later. Interestingly, a small overshoot can be seen during this drop in concentration.

The interplay between reactions 3−5 and reactions 8 and 9 is critical in accounting for the required feedback in this pH oscillator. The key intermediate in switching back and forth between these processes clearly is HOCl. After it is produced either directly or indirectly by reactions 8 and 9, it then switches on reactions 3−5. It is not coincidental that the calculations mentioned above show a change in [HOCl] of over 4 orders of magnitude during an oscillation.

$NaClO_2$−Na_2SO_3−H_2SO_4 System. The mechanism proposed for the chlorite−sulfite pH oscillator is given in Table 3, while corresponding rate equations and rate constants are shown in Table 4. The model includes reactions 1−9 (chlorite−sulfite subsystem A) from the chlorite−sulfite−carbonate pH oscillator, and reactions 13−22 (chlorite−sulfite subsystem B). Rate constants are known for most of the latter set of reactions, but

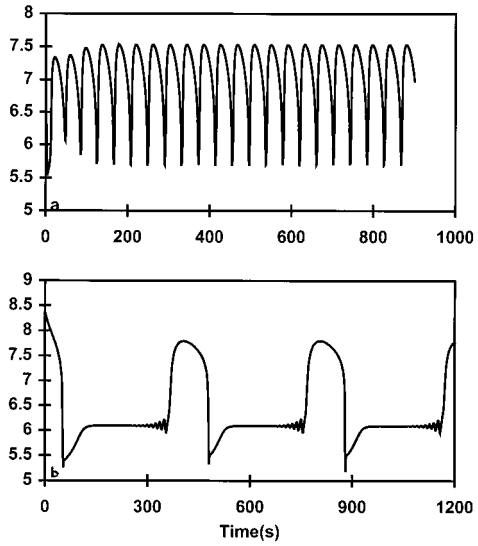

Figure 5. Calculated pH oscillations with experimental concentrations as in Figure 2, $k_0 = 1.70 \times 10^{-2}$ s^{-1}, and rate constants as in Table 4(a); and with experimental concentrations as in Figure 3, $k_0 = 1.00 \times 10^{-2}$ s^{-1}, and rate constants as in Table 4, except $k_{13} = 9.90 \times 10^8$ M^{-1} s^{-1}, $k_{17} = 1.82 \times 10^5$ M^{-1} s^{-1}, and $k_{18} = 4.45 \times 10^8$ M^{-1} s^{-1} (b).

not for reactions 13, 14, 17, and 18. These k values are estimated by numerical simulation, as described below. A number of different reactions provide feedback to replace that furnished by the carbonate subsystem. It should be noted that the chlorite−sulfite pH oscillator requires a lower [H$^+$] than in the presence of carbonate, so not as much negative feedback is needed.

Reaction 13, involving another Cl^+ transfer from HOCl to sulfur (in $ClSO_3^-$), is a key step, initiating a series of reactions to generate several important intermediates. Elemental Cl_2 formed in reaction 14 produces HOCl and Cl_2O_2 in reactions 15 and 16, respectively. Another source of Cl_2O_2 is reaction 17, which also plays the important role of providing feedback in one of the main reactants, SO_3^{2-}. In reactions 18 and 19, Cl_2O_2 reacts with both major reactants to form, respectively, HOCl and the free-radical intermediate, $^{\bullet}ClO_2$.

Chlorine dioxide has been found to play a significant role in other chlorite oscillators. In the present case, it reacts reversibly with sulfite in reaction 20 to give another radical intermediate, $SO_3^{\bullet-}$, and to provide feedback in the other main reactant, ClO_2^-.[22,24] Finally, the $SO_3^{\bullet-}$ radical anions can dimerize (reaction 21) or react together to produce HSO_3^- and H^+ (reaction 22).[25] Other reactions, such as that of $^{\bullet}ClO_2$ with $SO_3^{\bullet-}$, certainly are possible.

Simulations based on the rate equations and rate constants in Table 4 are shown in Figure 5a. Oscillations in pH are calculated for the same conditions as those used experimentally (see Figure 2). As with the carbonate-based system, the general features are reproduced, although not quantitatively. The k_0 range for simulated pH oscillations agrees reasonably well with experiment, but the periods tend to be rather long, especially at higher flow rates. The model in Table 3 has proved to be useful also for predicting the reactant concentrations required to produce oscillations in experiments. Thus far, it appears to be more reliable for this purpose in the middle range of reactant concentrations than at the extremes.

The experimental oscillations shown in Figure 3 can be simulated reasonably well using the rate constants in Table 4. However, in order to obtain the bursting effect, the rate constants k_{13}, k_{17}, and k_{18} need to be adjusted. The resulting simulation is shown in Figure 5b, along with the rate constant values used. While the qualitative features of the bursting are reproduced, this set of rate constants does not give as good a correlation with experimental k_0 ranges, periods of oscillation, or predicted reactant concentrations producing oscillations.

Attempts also were made to simulate the oscillations in batch referred to above. Using the conditions described in Figure 4 and the rate constant values given in Table 4, it was possible to reproduce the approximate pH changes and time scale for reaction. However, only inflections in the pH−time curve were obtained, but not oscillations. It is reasonable to expect that further refinements in the model, or improvements in the adjustable rate constant values, ultimately may lead to successful simulation of oscillations in a closed system.

When concentrations of key species are calculated from the rate equations and rate constants in Table 4, an interesting observation can be made. The concentration of $^{\bullet}ClO_2$ increases greatly (approaching 10^{-5} M) during an oscillation, even more so than [HOCl]. Using the rate constants in Table 4, we find [$^{\bullet}ClO_2$] increases by more than 3 orders of magnitude; with the adjusted k values used in Figure 5b, the increase is more than 5 orders of magnitude. In the latter case, $^{\bullet}ClO_2$ is also the species undergoing the greatest fluctuation during the rapid-oscillation phase in the bursting phenomenon. Other species showing significant fluctuation are HOCl and the proposed intermediate Cl_2SO_3. It appears that chlorine dioxide plays an important role in this chlorite oscillator as in some others previously reported.

Comparison to ClO_2^-−I^- Reaction. Because the chlorite-iodide system is perhaps the best understood of the chlorite oscillators, it was thought to be useful to compare it to the present system. Let us consider first Chlorite-Sulfite Subsystem A. Although it is difficult to draw an exact parallel between the ClO_2^-−I^- and ClO_2^-−SO_3^{2-} reactions, they do have in common the production of Cl(I) as either HOCl or OCl^-. The most striking parallel, however, comes in comparing the reactions of HOCl with I^- and SO_3^{2-}.

In addition to the mechanistic study done on the HOCl−SO_3^{2-} system referred to above,[23] Margerum et al.[26] have thoroughly investigated the mechanism of the HOCl−I^- reaction. They have shown that similar reversible Cl^+ transfer reactions involving HOCl occur with both I^- and SO_3^{2-}, forming $HOClI^-$ and $HOClSO_3^{2-}$, respectively. The iodide reaction, along with measured rate constants, is

$$HOCl + I^- \leftrightarrow HOClI^-; \quad k_{3'} = 4.3 \times 10^8 \text{ M}^{-1} \text{ s}^{-1}; \; k_{-3'} = 1.9 \times 10^6 \text{ s}^{-1} \quad (3')$$

Comparing rate constants for the parallel reactions, we see that k_3 (given in Table 2) is more than an order of magnitude greater than $k_{3'}$, consistent with the fact that SO_3^{2-} is a better nucleophile than I^-.

Margerum et al.[26] propose that $HOClI^-$ decomposes to form a new intermediate ICl, which then undergoes a rather slow, reversible hydrolysis reaction.

$$HOClI^- \rightarrow ICl + OH^-; \quad k_{4'} = 9(\pm 3) \times 10^5 \text{ s}^{-1} \quad (4')$$

$$ICl + H_2O \leftrightarrow HOI + Cl^- + H^+; \quad k_{5'} = 1.0 \times 10^2 \text{ s}^{-1}; \; k_{-5'} = 1 \times 10^6 \text{ M}^{-2} \text{ s}^{-1} \quad (5')$$

Again comparing to parallel reactions involving SO_3^{2-}, we note that k_4 and $k_{4'}$ are of the same order of magnitude, as are k_5 and $k_{5'}$. One difference between reactions 5 and 5′, however, is that reaction 5 is not reversible since the highly stable SO_4^{2-} is formed.

Going on to chlorite−sulfite subsystem B, we see that the sum of reactions 13 and 14 can be represented by the net reaction

$$ClSO_3^- + HOCl \rightarrow Cl_2 + SO_4^{2-} + H^+ \qquad (13'')$$

Reaction 13″ can be compared to the corresponding reaction involving iodide.

$$ICl + HOCl \rightarrow Cl_2 + HOI; \quad k_{13'} = 3 \times 10^4\ M^{-1}\ s^{-1} \qquad (13')$$

Based on relative rate constants, the difference in reactivity with HOCl between ICl and $ClSO_3$- appears to be much greater than between I^- and SO_3^{2-}.

Another comparison that can be made is in the reaction between Cl_2O_2 and reductant to regenerate HOCl. Reaction 18 involving SO_3^{2-} can be compared to the proposed reaction of Cl_2O_2 with I_2 as reductant[27]

$$Cl_2O_2 + I_2 + 2H_2O \rightarrow 2HOCl + 2HOI; \qquad k_{18'} = 1 \times 10^5\ M^{-1}\ s^{-1} \qquad (18')$$

The order of magnitude of k_{18} required in our simulations suggests that SO_3^{2-} is much more reactive toward Cl_2O_2 than is I_2.

Comparison to $^{\bullet}ClO_2-I^-$ Reaction. In chlorite−sulfite subsystem B, chlorine dioxide is produced from Cl_2O_2 and ClO_2^- in reaction 19. This reaction is not considered essential to the chlorite−iodide oscillator, but does play a role if ClO_2^- is in large excess. If one starts with $^{\bullet}ClO_2$, or if a significant amount of it is produced by reaction 19, the following reaction with I^- becomes important:

$$^{\bullet}ClO_2 + I^- \rightarrow ClO_2^- + {}^1/_2I_2; \quad k_{20'} = 6 \times 10^3\ M^{-1}\ s^{-1} \qquad (20')$$

The parallel reaction of $^{\bullet}ClO_2$ with SO_3^{2-} is reaction 20. One difference between the reactions is that reaction 20 is found to be reversible, while in the model for the $^{\bullet}ClO_2-I^-$ oscillator, the complicated kinetics of the reverse of reaction 20′ are not included. Another difference is that k_{20} for the sulfite reaction[22] is nearly 500 times as large as $k_{20'}$. Finally, it is noted that the product of reaction 20′ is molecular (I_2), rather than a radical anion ($SO_3^{\bullet-}$) as in reaction 20. However, assuming that $I^{\bullet}$ is actually formed instead of $^1/_2I_2$ in reaction 20′ and that two $I^{\bullet}$ radicals then combine very rapidly in reaction 21′,[28] the overall stoichiometry can be compared directly to that obtained in the case of reactions 20 and 21 for sulfite.

$$I^{\bullet} + I^{\bullet} \rightarrow I_2; \quad k_{21'} = 1 \times 10^9\ M^{-1}\ s^{-1} \qquad (21')$$

It was mentioned above that bursting behavior was observed under certain conditions, such as in Figure 3. We believe this is likely due mainly to the $^{\bullet}ClO_2-SO_3^{2-}$ reaction. Precedent for this conclusion is to be found with the $^{\bullet}ClO_2-I^-$ reaction in a CSTR.[29] Injection of superthreshold amounts of either chlorite ion or chlorine dioxide resulted in transient oscillations following a period of very low [I^-]. With periodic stimulation, bursts of oscillations are produced resembling those found in neurons. This can be accomplished by physical or chemical coupling, or by reciprocal stimulation, a method intended to be an approximation of mutual inhibitory synaptic connection.[30]

The simulation in Figure 5b shows qualitatively what is observed experimentally in Figure 3. Regular alternating periods of large-amplitude oscillations and small, rapid oscillations are found. This suggests either chemical coupling of two or more subsystems, each of which is capable of independent oscillations, or else production of superthreshold amounts of ClO_2^- or $^{\bullet}ClO_2$ which periodically stimulates the system to produce bursts of oscillations. The calculations referred to above show that large fluctuations in $^{\bullet}ClO_2$ occur during oscillations, thus making this the most likely species responsible if the latter scenario holds.

TABLE 5: General Model for Chlorite Ion Based Chemical Oscillators

no.	reaction
(M1)	$ClO_2^- + R + H^+ \rightarrow HOCl + RO$
(M2)	$ClO_2^- + HOCl + H^+ \rightarrow Cl_2O_2 + H_2O$
(M3)	$Cl_2O_2 + R + H_2O \rightarrow 2HOCl + RO$
(M4)	$HOCl + R \rightarrow RO + Cl^- + H^+$
(M5)	$Cl_2O_2 + ClO_2^- \rightarrow 2^{\bullet}ClO_2 + Cl^-$
(M6)	$Cl_2O_2 + H_2O \rightarrow ClO_3^- + Cl^- + 2H^+$

rate equations	rate constants at 25 °C
$R_{M1} = k_{M1}[ClO_2^-][R]$	$k_{M1}{}^a = 0.1\ M^{-1}\ s^{-1}$
$R_{M2} = k_{M2}[ClO_2^-][HOCl]$	$k_{M2}{}^a = 1 \times 10^4\ M^{-1}\ s^{-1}$
$R_{M3} = k_{M3}[Cl_2O_2][R]$	$k_{M3} = 2 \times 10^5\ M^{-1}\ s^{-1}$
$R_{M4} = k_{M4}[HOCl][R]$	$k_{M4} = 1 \times 10^4\ M^{-1}\ s^{-1}$
$R_{M5} = k_{M5}[Cl_2O_2][ClO_2^-]$	$k_{M5}{}^b = 2 \times 10^4\ M^{-1}\ s^{-1}$
$R_{M6} = k_{M6}[Cl_2O_2]$	$k_{M6} = 10.5\ s^{-1}$

[a] These rate constants include a constant proton concentration. [b] Corrected as in ref 17.

Comparison to General Model. In addition to the above comparisons to specific reactions involving iodide ion, it is useful to compare our proposed mechanism to the general model of Rabai and Orban.[17] The general model for chlorite-based oscillators can result in oscillations and chaos for certain values of rate constants, reactant concentrations, and flow rate. This model has been analyzed subsequently by Epstein et al.[31] over a wide range of parameters. Unlike the proposed mechanism for the chlorite−iodide oscillator, where iodide ions play the critical role and chlorite ions a secondary one, the general model assumes the feedback process originates from the chlorite. A summary of the reactions proposed in the general model is given in Table 5, along with corresponding rate equations.

Reaction M1, where $R = SO_3^{2-}$, can be compared to the sum of reactions 1 and 2 in Table 1. Both involve a slow step having the main function of initiating the autocatalytic path producing HOCl. One important difference is that the general model does not allow for autocatalysis in H^+, while chlorite−sulfite subsystem A in our model does. Reaction M2 was considered also in our model, but was not included since it had no significant effect on the simulations. Apparently, reactions 16 and 17 in Table 3 are much more important sources of intermediate Cl_2O_2 than is reaction M2.

A good comparison can be made between reaction M3 of the general model and reaction 18 in chlorite−sulfite subsystem B. The specific rate constant values used for these reactions have a significant effect on the predicted dynamical behavior in both models. Whereas simulations for the general model used a k_{M3} value of $1 \times 10^5\ M^{-1}\ s^{-1}$, we found it necessary to use a k_{18} value about 3 orders of magnitude larger. Since the value of k_{M3} is acknowledged to be dependent upon the specific reductant R, this is not necessarily an inconsistency.

Reaction M4, considered an important step in the general model, has the same stoichiometry as the sum of reactions 3, 4, and 5 in our model. The analogy falls short though, since M4 is considered an elementary step. Also, the value of k_{M4} needs to be relatively low ($1 \times 10^4\ M^{-1}\ s^{-1}$) so that the supply of HOCl is not depleted, thus terminating the autocatalytic cycle. This is in contrast to our model, where the autocatalytic cycle is preserved by means of the rather slow hydrolysis reaction

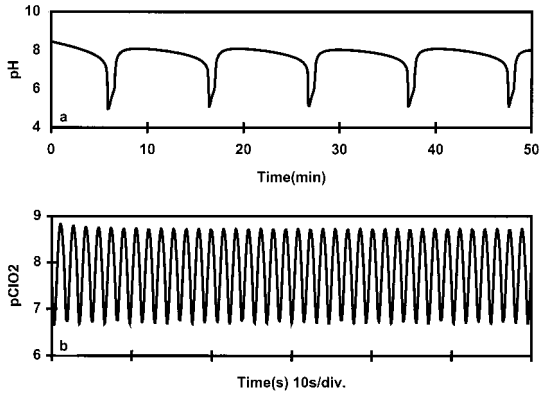

Figure 6. Calculated pH oscillations for core I oscillator with experimental concentrations as in Figure 3, $k_0 = 2.00 \times 10^{-3}$ s^{-1}, and rate constants as in Table 4, except $k_{13} = 3 \times 10^9$ M^{-1} s^{-1} (a); and calculated $pClO_2$ oscillations for core II oscillator with $[ClO_2^-]_0 = 3.50 \times 10^{-3}$ M, $[SO_3^{2-}]_0 = 1.15 \times 10^{-3}$ M, $[H^+]_0 = 1.20 \times 10^{-4}$ M, $k_0 = 2.00 \times 10^{-3}$ s^{-1}, and rate constants as in Table 4(b).

involving $ClSO_3^-$. Further, significant amounts of HOCl are regenerated directly or indirectly by reactions 8, 9, and 15 in our model.

The formation of $^\bullet ClO_2$ by reaction of Cl_2O_2 and ClO_2^- is considered to be important in both models (cf. reactions M5 and 19). One difference, however, is in the rate constant values used. The general model assumes a value of 2×10^4 M^{-1} s^{-1} for k_{M5}, whereas we base our value for k_{19} on the conclusion by Peintler et al.[32] that $k_{M5}/k_{M6} = 5.4 \times 10^4$ M^{-1}, where $k_{M6} = 1-10$ s^{-1}. We assumed a k_{M6} value of 1 s^{-1} in estimating k_{19} to be 5.4×10^4 M^{-1} s^{-1}.

Reaction M6 corresponds to the hydrolysis of Cl_2O_2 in a disproportionation reaction giving ClO_3^- and Cl^-, along with H^+. Calculations showed that this reaction could be omitted from our model without significantly affecting the simulated behavior of the system.

Chemical Coupling. The bursting behavior resulting from periodic stimulation of the $^\bullet ClO_2-I^-$ reaction, such as when two CSTRs are physically coupled, was discussed above. One of the best understood systems involving chemically coupled oscillators is that of $BrO_3^- - ClO_2^- - I^-$ in a CSTR.[33] With chemical coupling, two or more subsystems independently capable of giving oscillations are linked through a common species, in a single vessel.

Although the $ClO_2^- - SO_3^{2-} - H^+$ system may at first seem too simple for chemical coupling to occur, we have devised two subsystems which in principle are capable of independent oscillations. The core I oscillator consists of chlorite−sulfite subsystem A, along with reactions 13 and 14 of chlorite−sulfite subsystem B. Note that this oscillator does not require the presence of $^\bullet ClO_2$. Simulations using this model are shown in Figure 6a for the same reactant concentrations as in Figure 3, but with $k_0 = 2.00 \times 10^{-3}$ s^{-1}. The same rate constant values as in Table 4 were used, except that k_{13} was increased to a value approaching the diffusion-controlled limit (3×10^9 M^{-1} s^{-1}). This subsystem gives pH oscillations similar to those found experimentally, except they are of significantly lower frequency.

The core II oscillator consists of all but reactions 8 and 9 of chlorite−sulfite subsystem A, and all of chlorite−sulfite subsystem B. Because two of the main reactions responsible for positive feedback in H^+ now have been omitted from the overall mechanism in Table 3, pH oscillations are not obtained, but oscillations in $pClO_2$ do occur. Simulations based on this model are shown in Figure 6b under the conditions given there, using the same rate constants as in Table 4. The very small period of ca. 1.5 s (similar to that observed in the batch reaction) for the $pClO_2$ oscillations is striking. We suggest the possibility that the complex oscillations observed experimentally in Figure 3 may be attributed to coupling of two core oscillators—the low-frequency pH oscillator and the high-frequency $pClO_2$ oscillator. The former accounts for the large-amplitude oscillations and the latter accounts for the small, rapid oscillations in the bursting phenomenon.

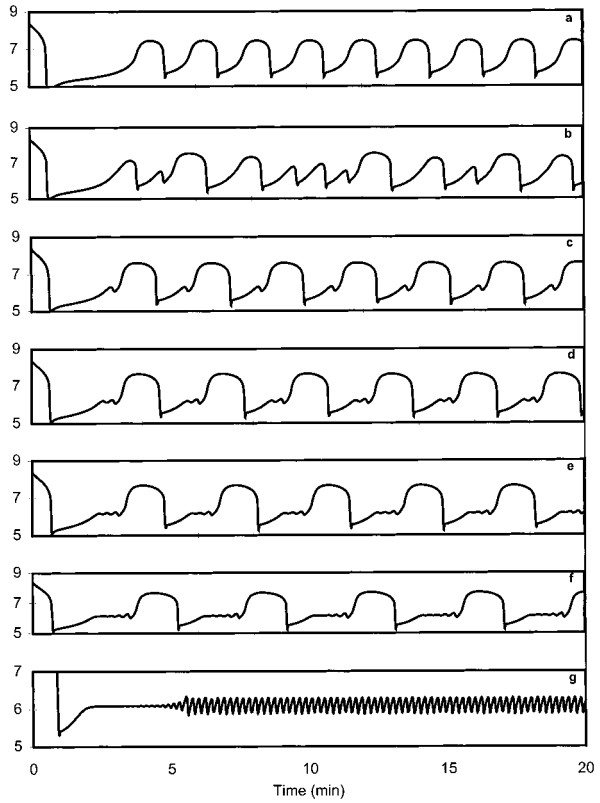

Figure 7. Calculated pH oscillations with experimental concentrations as in Figure 3 and rate constants as in Figure 5b. $k_0 \times 10^3$, s^{-1}: 3.00 (a); 4.07 (b); 4.50 (c); 5.25 (d); 5.85 (e); 6.40 (f); 10.5 (g).

One type of complex behavior shown by physically coupled systems, such as the $^\bullet ClO_2-I^-$ reaction, and by systems which are chemically coupled, such as that of $BrO_3^- - ClO_2^- - I^-$, is the phenomenon of period-adding. This involves a regular increase in the number of small oscillations following the large one, as an experimental parameter such as k_0 is changed. Interestingly, it is possible to simulate such behavior in the case of the present system.

Figure 7 shows simulated pH oscillations under the same experimental conditions as in Figure 3. The specific rate constant values used are the same as in Figure 5. As the value of k_0 is increased regularly, the period-adding effect is very clear. Note that apparently chaotic behavior (panel b) is shown as part of this sequence. This is similar to what was found with the $BrO_3^- - ClO_2^- - I^-$ system.[34] One difference between the systems, however, is that the latter shows period-adding as k_0 is decreased, whereas in our system period-adding requires that k_0 be increased.

Another type of complex behavior suggested by the simulations in Figures 5b and 7 is that of compound oscillations. These occur when one small-amplitude oscillation appears to be tacked onto each large-amplitude one. Further, in Figure 7 one observes a very unusual feature also shown by the $BrO_3^- - ClO_2^- - I^-$ system. This involves periodic behavior consisting of one compound oscillation C_n followed by n small-amplitude oscillations.

Conclusions

To summarize, this work has resulted in several new discoveries. Our original goal of constructing a new homogeneous carbonate-based pH oscillator was achieved. We also have added to the list of known chlorite-based oscillators. More specifically, we report here the first chlorite-based pH oscillator. Depending on one's approach to the taxonomy of chemical oscillators, one could perhaps make the case that the chlorite−sulfite pH oscillator represents a new subclass of chlorite oscillator. However, as mentioned above, a chlorite-based oscillator involving IO_3^- or I_2 as an oxidant and SO_3^{2-} as a reductant was first discovered nearly 20 years ago.[20] One thing that seems clear is that the $ClO_2^- - SO_3^{2-}$ system represents a new minimal or prototype chlorite oscillator, taking its place alongside the $ClO_2^- - I^-$ oscillator.

In spite of the complexity of the nonlinear dynamics found in the chlorite−sulfite system, this may be the simplest, and best understood mechanistically, sulfur-based chlorite oscillator. Perhaps in the future it may help account for the behavior of other sulfur-based chlorite oscillators (e.g., with S^{2-}, SCN^-, $S_2O_3^{2-}$, or TU). One other benefit of the present study is the introduction of new reactions involving sulfur and chlorine species and the suggestion of the existence of a new intermediate, Cl_2SO_3. It has also provided the incentive for the measurement, or at least the estimation, of previously unknown rate constants. Finally, in terms of the basic components, the chlorite−sulfite pH oscillator may be the simplest "single oscillator" to demonstrate chemical coupling.

Future Directions

Although a great deal has been learned about how this pH oscillator works, there is much more to be done. Further CSTR studies over a wide range of reactant concentrations are needed to obtain the phase diagram(s) necessary to characterize fully the various types of behavior observed in this system. Further, it will be useful to investigate the batch reaction under additional conditions, such as with lower reactant concentrations where the reaction is slower, to confirm that it represents what would be the first pH oscillator in a closed system. The above work is presently underway in our laboratory.

The simulated period-adding effect involving compound oscillations and possible chaos shown in Figure 7 suggests that a systematic search for such experimental behavior would be in order. The apparent chemical coupling in our system also suggests investigations of the core oscillators proposed above. The subsystem involving pH oscillations could be studied under conditions where the role of $^\bullet ClO_2$ is insignificant. This implies the possibility of observing pH oscillations where ClO_2^- is not in large excess over SO_3^{2-}, or perhaps even where sulfite is in excess. On the other hand, the subsystem involving oscillations in $pClO_2$ (but not in pH) could be studied under rather acidic conditions, where buffering occurs, and with a very large excess of ClO_2^-. The latter subsystem also suggests the possibility of finding a new chemical oscillator involving SO_3^{2-} (in a CSTR if not in batch), where $^\bullet ClO_2$ is substituted for ClO_2^- as one of the principal components. Considering the parallel with the $^\bullet ClO_2 - I^-$ reaction as described above, this would not be surprising.

It should be pointed out that it may not be possible to observe experimental oscillations for one or both core oscillators, even though simulations show otherwise. An example of this is the hydrogen peroxide−thiosulfate−sulfite flow system.[35] One of the core oscillators found to give calculated pH oscillations involves the $H_2O_2 - S_2O_3^{2-}$ subsystem. However, no oscillations can be found experimentally under isothermal conditions. Only in the presence of a catalytic amount of Cu^{2+} are pH oscillations observed.

One obvious area for future study involving the chlorite−sulfite system is that of spatiotemporal oscillations. Such behavior has been observed with both the chlorite−iodide−malonic acid (CIMA) and chlorine dioxide−iodide−malonic acid (CDIMA) reactions.[36,37] Both of these systems also show oscillations in batch. The similarities between sulfite and iodide in their reactions with chlorite, as mentioned above, suggest the possibility of obtaining such phenomena as Turing patterns and propagating pH fronts with the sulfite-based system. This seems especially likely because of the feedback processes regenerating S(IV) species in our proposed mechanism. The main purpose of the malonic acid in the CIMA and CDIMA reactions is to regenerate I^-. If spatiotemporal phenomena can be observed with the chlorite−sulfite reaction, this system would seem to have a clear advantage over the CIMA and CDIMA reactions for future studies in terms of the simplicity of both the components and the mechanism.

Acknowledgment. G.A.F. acknowledges that this research was supported by an award from Research Corporation. G.A.F. also expresses gratitude to the Department of Chemistry and Biochemistry at South Dakota State University, where much of the manuscript was written while on sabbatical leave. We wish to thank Joseph Turner and, especially, C. Wayland Rushing, for invaluable assistance. Finally, we acknowledge helpful discussions with Richard J. Field, Qingyu Gao, and Gyula Rabai.

References and Notes

(1) Orban, M.; Epstein, I. R. *J. Am. Chem. Soc.* **1985**, *107*, 2302.
(2) Giannos, S. A.; Dinh, S. M.; Berner, B. *J. Pharm. Sci.* **1995**, *84*, 539.
(3) Siegel, R. A.; Zou, X.; Baker, J. P. *Proc. Int. Symp. Controlled Release Bioact. Mater.* **1996**, *23*, 115.
(4) Yoshida, R.; Ichijo, H.; Hakuta, T.; Yamaguchi, T. *Macromol. Rapid Commun.* **1995**, *16*, 305.
(5) Luo, Y.; Epstein, I. R. *J. Am. Chem. Soc.* **1991**, *113*, 1518.
(6) Rabai, Gy.; Orban, M.; Epstein, I. R. *Acc. Chem. Res.* **1990**, *23*, 258.
(7) Vanag, V. K. *J. Phys. Chem.* **1998**, *102*, 601.
(8) Rabai, Gy.; Hanazaki, I. *J. Phys. Chem.* **1996**, *100*, 15454.
(9) Rabai, Gy. *J. Phys. Chem.* **1997**, *101*, 7085.
(10) Frerichs, G. A.; Thompson, R. C. *J. Phys. Chem. A* **1998**, *102*, 8142.
(11) Orban, M.; Epstein, I. R. *J. Phys. Chem.* **1982**, *86*, 3907.
(12) Alamgir, M.; Epstein, I. R. *J. Phys. Chem.* **1985**, *89*, 3611.
(13) Orban, M. *React. Kinet. Catal. Lett.* **1990**, *42*, 333.
(14) Alamgir, M.; Epstein, I. R. *Int. J. Chem. Kinet.* **1985**, *17*, 429.
(15) Halperin, J.; Taube, H. *J. Am. Chem. Soc.* **1952**, *74*, 375.
(16) Edblom, E. C.; Luo, Y.; Orban, M.; Kustin, K.; Epstein, I. R. *J. Phys. Chem.* **1989**, *93*, 2722.
(17) Rabai, Gy.; Orban, M. *J. Phys. Chem.* **1993**, *97*, 5935.
(18) Epstein, I. R.; Pojman, J. A. *An Introduction to Nonlinear Dynamics: Oscillations, Waves, Patterns, and Chaos*; Oxford University Press: New York, 1998.
(19) De Kepper, P.; Epstein, I. R.; Kustin, K. *J. Am. Chem. Soc.* **1981**, *103*, 2133.
(20) Orban, M.; De Kepper, P.; Epstein, I. R.; Kustin, K. *Nature* **1981**, *292*, 816. Orban, M.; Dateo, C.; De Kepper, P.; Epstein, I. R. *J. Am. Chem. Soc.* **1982**, *104*, 5911.
(21) Lengyel, I.; Li, J.; Kustin, K.; Epstein, I. R. *J. Am. Chem. Soc.* **1996**, *118*, 3708.
(22) Rushing, C. W.; Thompson, R. C., unpublished data.
(23) Yiin, B. S.; Margerum, D. W. *Inorg. Chem.* **1988**, *27*, 1670. Fogelman, K. D.; Walker, D. M.; Margerum, D. W. *Inorg. Chem.* **1989**, *28*, 986.
(24) Merenyi, G.; Lind, J.; Shen, X. *J. Phys. Chem.* **1988**, *92*, 134.
(25) Fischer, M.; Warneck, P. *J. Phys. Chem.* **1996**, *100*, 15111.
(26) Kumar, K.; Day, R. A.; Margerum, D. W. *Inorg. Chem.* **1986**, *25*, 4344. Nagy, J. C.; Kumar, K.; Margerum, D. W. *Inorg. Chem.* **1988**, *27*, 2773.

(27) Rabai, G.; Beck, M. T. *Inorg. Chem.* **1987**, *26*, 1195.
(28) Marlovits, G.; Wittmann, M.; Nosticzius, Z.; Gaspar, V. *J. Phys. Chem.* **1995**, *99*, 5359.
(29) Dolnik, M.; Epstein, I. R. *J. Chem. Phys.* **1993**, *98*, 1149.
(30) Shepherd, G. H. *Neurobiology*; Oxford University Press: Oxford, UK, 1988.
(31) Lengyel, I.; Gyorgyi, L.; Epstein, I. R. *J. Phys. Chem.* **1995**, *99*, 12804.
(32) Peintler, G.; Nagypal, I.; Epstein, I. R. *J. Phys. Chem.* **1990**, *94*, 2954.
(33) Citri, O.; Epstein, I. R. *J. Phys. Chem.* **1988**, *92*, 1865.
(34) Alamgir, M.; Epstein, I. R. *J. Phys. Chem.* **1984**, *88*, 2848.
(35) Rabai, G.; Hanazaki, I. *J. Phys. Chem. A* **1999**, *103*, 7268.
(36) De Kepper, P.; Epstein, I. R.; Orban, M.; Kustin, K. *J. Phys. Chem.* **1982**, *86*, 170.
(37) Lengyel, I.; Kadar, S.; Epstein, I. R. *J. Phys. Chem.* **1992**, *69*, 2729.
(38) Harris, Daniel C. *Exploring Chemical Analysis*; W. H. Freeman & Co.: New York, 1997.